

November 16, 2015

Realization of adiabatic Aharonov-Bohm scattering with neutrons

Erik Sjöqvist*,^{1,2,*} Martin Almquist,³ Ken Mattsson,³ Zeynep Nilhan Gürkan,⁴ and Björn Hessmo^{5,6}

¹*Department of Quantum Chemistry, Uppsala University, Box 518, Se-751 20 Uppsala, Sweden*

²*Department of Physics and Astronomy, Uppsala University, Box 516, Se-751 20 Uppsala, Sweden*

³*Department of Information Technology, Uppsala University, Lägerhyddsvägen 2, Se-752 37 Uppsala, Sweden*

⁴*Department of Industrial Engineering, Gediz University, Seyrek, 35665, Menemen-Izmir, Turkey*

⁵*Centre for Quantum Technologies, National University of Singapore, 3 Science Drive 2, 117543 Singapore, Singapore*

⁶*Department of Physics, National University of Singapore, 3 Science Drive 2, 117543 Singapore, Singapore*

The adiabatic Aharonov-Bohm (AB) effect is a manifestation of the Berry phase acquired when some slow variables take a planar spin around a loop. While the effect has been observed in molecular spectroscopy, direct measurement of the topological phase shift in a scattering experiment has been elusive in the past. Here, we demonstrate an adiabatic AB effect by explicit simulation of the dynamics of unpolarized very slow neutrons that scatter on a long straight current-carrying wire.

PACS numbers: 03.65.Vf, 03.75.Be

I. INTRODUCTION

Aharonov and Bohm [1] pointed out that a charged quantum particle may acquire an observable phase shift by circling around a completely shielded magnetic flux. This remarkable effect is purely non-classical as the electromagnetic field vanishes at the location of the particle, which thereby experiences no Lorentz force. The origin of the phase shift is topological: it only depends on the winding number of the particle's path around the magnetic flux.

The original Aharonov-Bohm (AB) setup for electric charge belongs to a larger class of topological phase effects. This includes topological phase shifts arising for electrically neutral particles in certain electromagnetic configurations [2, 3] as well as in general quantum systems that undergo adiabatic evolution [4]. A paradigmatic example of the latter is a molecule that acquires an AB phase shift when it reshapes slowly around a conical intersection in nuclear configuration space [5]. This adiabatic AB effect is imprinted in the spectral properties related to the pseudorotational molecular motion, and has been observed [6] in the metallic trimer Na₃. It has further been predicted [7] in scattering-type chemical reactions, such as in the hydrogen exchange reaction H + H₂. Due to subtle cancellation effects, however, direct observation of the AB effect in molecular scattering has been elusive in the past [8–10].

Matter waves in spatially varying electromagnetic fields is a tool to engineer a wide range of quantum effects [11–13]. If the variation of these fields is sufficiently slow, the particle motion is governed by adiabatic gauge fields [14–16] similar to those in molecules and has been proposed to give rise to AB phase shifts under certain conditions [17, 18]. Here, we develop an adiabatic AB

effect for matter waves that scatter on a static inhomogeneous magnetic field produced by a current-carrying wire. The setup uses the quantum properties of neutrons to induce the AB effect. Earlier experimental demonstrations of other topological phase effects, such as the Aharonov-Casher [19] and scalar AB phase shifts [20], as well as related Berry phase induced spinor rotations [21, 22], have shown that neutrons are suitable to realize AB effects due to their robust internal structure, the ease of detecting them with almost 100 % efficiency, and their weak coupling to the environment. Our setup is similar to the one proposed in Ref. [23] for a nanoelectronic system.

II. PHYSICAL SETUP

Imagine a colimated beam of neutrons that scatter on a long straight wire of radius R , carrying an electrical current I_w . The resulting magnetic field is given by Biot-Savart's law

$$\mathbf{B} = \frac{\mu_0 I_w}{2\pi R} f(r) \mathbf{e}_\theta, \quad f(r) = \begin{cases} \frac{1}{r}, & r \geq 1, \\ r, & r < 1, \end{cases} \quad (1)$$

where we have assumed that the wire points along the z -axis and carries a uniform current density. Here, θ is the polar angle in cylindrical coordinates with corresponding basis vector \mathbf{e}_θ , r is the distance from the wire in units of R , and μ_0 is permeability of vacuum. The magnetic field induces a local energy splitting of the neutron spin states, as described by the Zeeman Hamiltonian $\mathcal{H} = -\boldsymbol{\mu} \cdot \mathbf{B} = -\mu \frac{1}{2} \boldsymbol{\sigma} \cdot \mathbf{B}$ with $\mu = -9.65 \cdot 10^{-27}$ J/T the neutron magnetic moment and $\boldsymbol{\sigma} = (\sigma_x, \sigma_y, \sigma_z)$ the standard Pauli operators representing the neutron spin. The eigenvalues of the Hamiltonian are $\pm \frac{|\mu| \mu_0 I_w}{4\pi R} f(r) \equiv \pm V_0 f(r)$, which introduce a potential energy barrier (well) of height V_0 (depth $-V_0$) at the surface of the wire.

The Hamiltonian relevant for the AB effect is given by the kinetic energy of the neutron in the xy plane, plus

* e-mail: erik.sjoqvist@kemi.uu.se

the Hamiltonian describing the neutron spin, i.e.,

$$H_{\text{tot}} = -\frac{\hbar^2}{2m} \nabla_{\mathbf{r}}^2 + \mathcal{H}. \quad (2)$$

We write the total wave function as $|\psi(\mathbf{r}, s)\rangle = \varphi_+(\mathbf{r}, s) |\chi_+(\theta)\rangle + \varphi_-(\mathbf{r}, s) |\chi_-(\theta)\rangle$, where $\mathbf{r} = (x, y) = r(\cos \theta, \sin \theta)$ and $|\chi_{\pm}(\theta)\rangle = \frac{1}{\sqrt{2}}(\mp i|\uparrow\rangle + e^{i\theta}|\downarrow\rangle)$ are the local spin eigenvectors with $\sigma_z|\uparrow\rangle = |\uparrow\rangle$, $\sigma_z|\downarrow\rangle = -|\downarrow\rangle$. The two spin eigenstates are associated with the potential energies $\pm V_0 f(r)$. Here, $s = \hbar t / (2mR^2)$ (dimensionless time) with $m = 1.67 \cdot 10^{-27}$ kg being the neutron mass.

To determine the spatial wave functions $\varphi_{\pm}(\mathbf{r}, s)$ we eliminate the spin degree of freedom by multiplying the Schrödinger equation with $\langle \chi_{\pm} |$ yielding the coupled equations

$$\begin{aligned} i\partial_s \varphi_{\pm}(\mathbf{r}, s) = & \left[-\partial_r^2 - \frac{1}{r} \partial_r \right. \\ & \left. - \frac{1}{r^2} \left(\partial_{\theta} + \frac{i}{2} \right)^2 \pm \kappa f(r) + \frac{1}{4r^2} \right] \varphi_{\pm}(\mathbf{r}, s) \\ & + \left(\frac{1}{2r^2} + i \frac{1}{r^2} \partial_{\theta} \right) \varphi_{\mp}(\mathbf{r}, s), \end{aligned} \quad (3)$$

where $\kappa = 2mR^2 V_0 / \hbar^2$.

The adiabatic regime is characterized by negligible Born-Huang potential $\frac{1}{4r^2}$ and off-diagonal coupling terms $(\frac{1}{2r^2} \pm i \frac{1}{r^2} \partial_{\theta}) \varphi_{\mp}(\mathbf{r}, s)$. For low neutron velocities, the wire is impenetrable and the validity of the adiabatic approximation can be checked by comparing the size of the scalar potential $\kappa f(r)$ and $1/r^2$ at the surface of the wire. This yields the adiabatic condition $\kappa \gg 1$. In this regime, it follows from Eq. (3) that the spatial wave packets $\varphi_{\pm}(\mathbf{r}, s)$ are separately determined by the effective Schrödinger equations

$$\begin{aligned} i\partial_s \varphi_{\pm}(\mathbf{r}, s) = & \left[-\partial_r^2 - \frac{1}{r} \partial_r \right. \\ & \left. - \frac{1}{r^2} (\partial_{\theta} + i\alpha)^2 \pm \kappa f(r) \right] \varphi_{\pm}(\mathbf{r}, s) \end{aligned} \quad (4)$$

where $\alpha/r = \frac{1}{2r}$ is the Mead-Berry vector potential pointing in the θ direction.

The shift $\partial_{\theta} \rightarrow \partial_{\theta} + i\alpha$ is the key origin of the AB effect. It originates from the adiabatic elimination of the spin, which introduces the Mead-Berry vector potential [4, 5] $\mathbf{A} = i \langle \chi_{\pm} | \nabla_{\mathbf{r}} | \chi_{\pm} \rangle = -(\alpha/r) \mathbf{e}_{\theta}$ in the kinetic energy of the neutron. This defines the effective magnetic flux

$$\Phi = \oint_C \mathbf{A} \cdot d\mathbf{x} = -2\pi\alpha = -\pi \quad (5)$$

picked up by the phase when the neutron moves around the wire along a loop C . Φ vanishes if the neutron does not encircle the wire. The vector potential thus corresponds to an AB flux line carrying half a flux unit (semi-fluxon) sitting at the conical intersection point at $r = 0$. The flux-induced phase is a topological property as it depends neither on the detailed shape of the loop C nor

on the dynamical parameters of the system, such as the electrical current I_w and the speed of the neutron. A consequence of the topological nature of the phase shift is that for a non-uniform electrical current density, we can predict that there must be an odd number of points at which the magnetic field vanishes inside the wire as each conical intersection carries half a flux unit [24, 25].

III. RESULTS

We numerically simulate an unpolarized neutron that scatters on the wire. We solve Eq. (4) for the two adiabatic channels and calculate the density profile

$$\rho(\mathbf{r}, s) = \frac{1}{2} (|\varphi_+(\mathbf{r}, s)|^2 + |\varphi_-(\mathbf{r}, s)|^2) \quad (6)$$

obtained by tracing over the spin. We choose $I_w = 10$ mA and $R = 10^{-5}$ m, which yields $\kappa = 29$. The spatial degree of freedom of the neutron is modeled as an incoming Gaussian wave packet of $\sim 20 \mu\text{m}$ width, whose centre is moving in the xy plane straight on to the wire at relative velocity v_{xy} . The wire is assumed to be made of an electrically conducting material with a positive neutron optical potential that can reflect slow neutrons. An appropriate choice would be copper with a positive optical potential corresponding to a critical neutron velocity of about 5.7 m/s. We assume neutron velocities v_{xy} well below this critical value, which means that we can take $\varphi_{\pm}(\mathbf{r}, s)$ to vanish at $r = 1$. With the chosen κ , we expect the adiabatic treatment to be valid, which has indeed been confirmed numerically to a high degree of accuracy by comparing the wave packet dynamics arising from Eqs. (4) and (3).

The summation-by-parts-simultaneous approximation term (SBP-SAT) method [26] is a time-stable well-proven high-order difference methodology suitable for solving high-order wave-dominated phenomena [27]. In the present study a sixth-order accurate SBP-SAT approximation has been employed, solving Eq. (4) with high fidelity.

To study the adiabatic AB effect we first compare the dynamics with $v_{xy} = 0.02$ m/s for $\alpha = \frac{1}{2}$ and $\alpha = 0$, where the latter case corresponds to ignoring the adiabatic flux. As seen in Fig. 1 (see also Supplementary Movies 1 and 2), the effective AB flux introduces a nodal line in the forward direction, which is not visible when $\alpha = 0$. This is the key signature of the adiabatic AB effect related to the effective flux line carrying half a flux unit associated with destructive interference in the forward direction [17, 18, 28]. It would be directly detectable by measuring the neutron density profile in the xy plane behind the wire. We further perform simulations at $v_{xy} = 0.03$ and 0.04 m/s, shown in Fig. 2. The nodal line persists, which demonstrates the nondispersive nature of the AB effect and opens up for the possibility to perform the test even if we allow for a distribution of incoming velocities within the adiabatic regime.

A significant simplification of the experimental setting is that unpolarized neutrons can be used, due to the

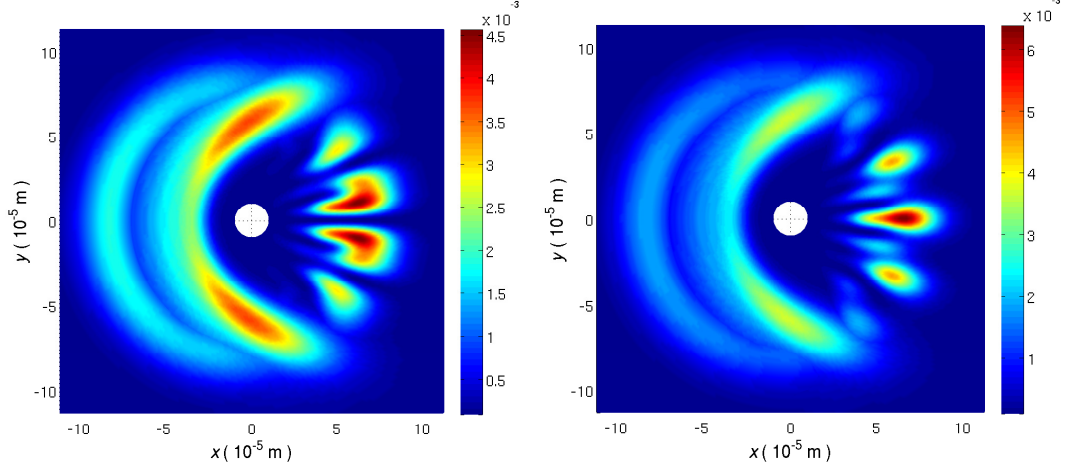


FIG. 1. Scattered density of unpolarized neutrons moving with incoming velocity 0.02 m/s perpendicular to a very long straight current-carrying wire. Left panel includes the adiabatic AB effect. Right panel neglects the adiabatic AB effect. The key difference is the AB-induced nodal line in the forward direction ($x > 0, y = 0$) that is absent when neglecting the AB effect. The wire represented by the white region around the origin has radius 10^{-5} m and carries 10 mA electrical current.

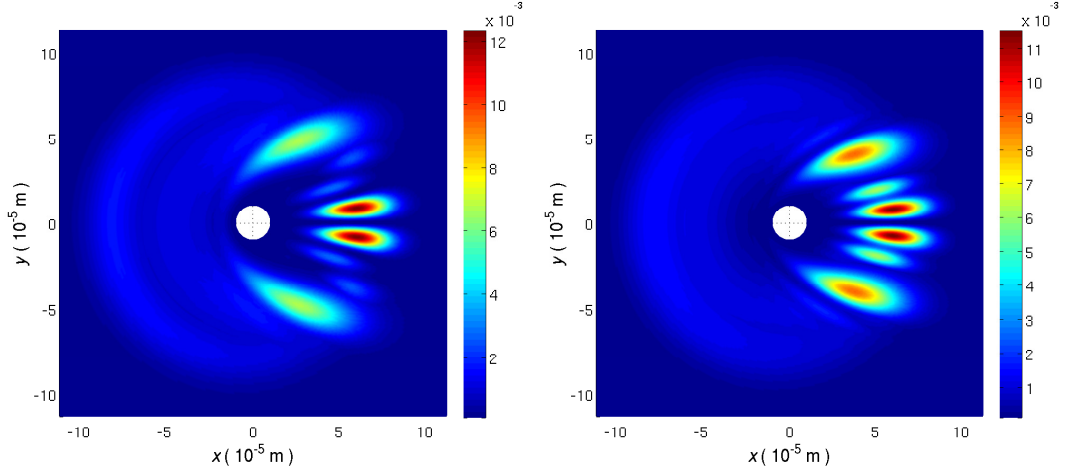


FIG. 2. Scattered density of unpolarized neutrons at incoming perpendicular incoming velocities 0.03 m/s (left panel) and 0.04 m/s (right panel) with the same wire radius and electrical current as in Fig 1. The nodal line is clearly visible demonstrating the nondispersive nature of the AB effect.

spatial bifurcation caused by the energy splitting of the two local spin eigenstates. We demonstrate this effect in terms of the local spin density

$$\begin{aligned} \boldsymbol{\sigma}(\mathbf{r}, s) &= \frac{1}{2} \left(|\varphi_+(\mathbf{r}, s)|^2 \langle \chi_+ | \boldsymbol{\sigma} | \chi_+ \rangle \right. \\ &\quad \left. + |\varphi_-(\mathbf{r}, s)|^2 \langle \chi_- | \boldsymbol{\sigma} | \chi_- \rangle \right) \\ &= \frac{1}{2} \left(|\varphi_+(\mathbf{r}, s)|^2 - |\varphi_-(\mathbf{r}, s)|^2 \right) \mathbf{e}_\theta. \end{aligned} \quad (7)$$

The scalar part $\frac{1}{2} \left(|\varphi_+(\mathbf{r}, s)|^2 - |\varphi_-(\mathbf{r}, s)|^2 \right)$ is shown Fig. 3 (see also Supplementary Movie 3). We note that only $|\chi_-(\theta)\rangle$ contributes significantly to the AB phase shift; the reason being the attractive nature of the adiabatic potential $-V_0 f(r)$ associated with this state for

$r > 1$.

The low neutron velocities can be experimentally achieved by letting the neutron hit the wire at small angle. This can be realized for cold neutrons (speed a few 100 m/s) initially moving parallel to a horizontal wire. The bending of the neutron beam in the gravitational field induces a small velocity component v_{xy} towards the wire. For fixed incoming speed, the relative velocity v_{xy} can be controlled either by moving the wire in the vertical direction or by tilting it slightly upwards in the direction of motion.

The incoming wave packet used in the numerical simulations have been chosen to clearly demonstrate the adiabatic AB effect on the spatial distribution of the scattered neutrons. However, to reproduce this wave packet

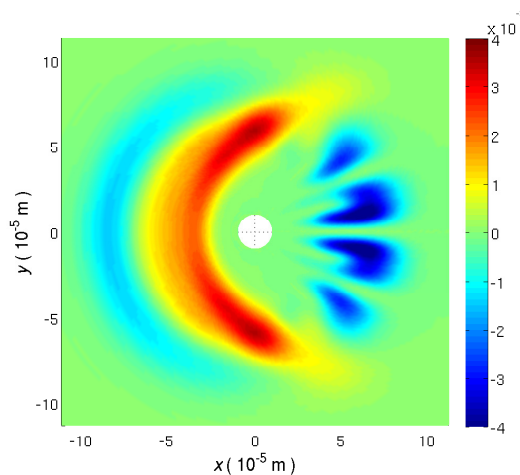


FIG. 3. **Local spin density of AB-scattered unpolarized neutrons.** The incoming perpendicular velocity of the neutrons is 0.02 m/s with the same wire radius and electrical current as in Fig 1. Due to the attractive (repulsive) scalar potential felt by the local spin down (up) state, the measurable AB effect is fully dominated by the spin down state.

dynamics in an actual experiment would be challenging as it would require a very high angular resolution and precise centering of the neutron beam. The difficulty is associated with the small size of the wave packet that would decrease the number of neutrons that would hit the wire in the desired manner. A less demanding setting would require the transversal width of the wave packet to be much larger than the width of the wire as this would allow for higher neutron flux. The AB-induced destructive interference effect in the forward direction would be intact for such a wave packet, as the AB effect is topological and therefore independent of shape and size of the neutron wave function.

IV. CONCLUSIONS

We have demonstrated an adiabatic AB effect for slow neutrons that scatter on a magnetic field produced by an

electrical current through a very long wire. The mechanism of the effect is the Berry phase of the neutron spin restricted to the plane perpendicular to the wire. Therefore, the acquired phase shift is restricted to π , known to be the only possible non-trivial value of a planar spin. The π phase shift causes destructive interference in the forward direction, providing an unambiguous signature of the adiabatic AB effect in a scattering setup. We have further demonstrated the nondispersive nature of the effect, which opens up for the possibility to observe the effect for higher neutron velocities in the adiabatic regime.

ACKNOWLEDGMENTS

E. S. acknowledges support from the Swedish Research Council through Grant No. D0413201. B. H. was supported by the National Research Foundation and the Ministry of Education (Singapore).

-
- [1] Y. Aharonov and D. Bohm, *Significance of electromagnetic potentials in the quantum theory*, Phys. Rev. **115**, 485 (1959).
 - [2] Y. Aharonov and A. Casher, *Topological quantum effects for neutral particles*, Phys. Rev. Lett. **53**, 319 (1984).
 - [3] H. Wei, R. Han, and X. Wei, *Quantum phase of induced dipoles moving in a magnetic field*, Phys. Rev. Lett. **75**, 2071 (1995).
 - [4] M. V. Berry, *Quantal phase factors accompanying adiabatic changes*, Proc. R. Soc. London, Ser. A **329**, 45 (1984).
 - [5] C. A. Mead, *The molecular Aharonov-Bohm effect*, Chem. Phys. **49**, 23 (1980).
 - [6] H. von Busch, V. Dev, H.-A. Eckel, S. Kasahara, J. Wang, W. Demtröder, P. Sebald, and W. Meyer, *Unambiguous proof for Berry's phase in the sodium trimer: analysis of the transition $A^2E'' \leftarrow X^2E'$* , Phys. Rev. Lett. **81**, 4584 (1998).
 - [7] B. Lepetit and A. Kuppermann, *Numerical study of the geometric phase in the H+H₂ reaction*, Chem. Phys. Lett. **166**, 581 (1990).
 - [8] B. K. Kendrick, *Geometric phase effects in chemical reaction dynamics and molecular spectra*, J. Phys. Chem. **107**, 6739 (2003).
 - [9] J. Jankunas, M. Sneha, R. N. Zare, F. Bouakline, and S. C. Althorpe, *Hunt for the geometric phase effects in H + HD \rightarrow HD(ν' , j') + H*, J. Chem. Phys. **139**, 144316 (2013).
 - [10] J. Juanes-Marcos, S. C. Althorpe, and E. Wrede, *Theoretical study of geometric phase effects in the hydrogen-*

- exchange reaction*, Science **309**, 1227 (2005).
- [11] S.-L. Zhu, H. Fu, C.-J. Wu, S.-C. Zhang, and L.-M. Duan, *Spin Hall effects for cold atoms in a light-induced gauge potential*, Phys. Rev. Lett. **97**, 240401 (2006).
 - [12] G. Juzeliūnas, J. Ruseckas, A. Jacob, L. Santos, and P. Öhberg, *Double and negative reflection of cold atoms in non-Abelian gauge potentials*, Phys. Rev. Lett. **100**, 200405 (2008).
 - [13] J. Y. Vaishnav and C. W. Clark, *Observing zitterbewegung with ultracold atoms*, Phys. Rev. Lett. **100**, 153002 (2008).
 - [14] J. Ruseckas, G. Juzeliūnas, P. Öhberg, and M. Fleischhauer, *Non-Abelian gauge potentials for ultracold atoms with degenerate dark states*, Phys. Rev. Lett. **95**, 010404 (2005).
 - [15] Y.-J. Lin, R. L. Compton, K. Jiménez-García, J. V. Porto, and I. B. Spielman, *Synthetic magnetic fields for ultracold neutral atoms*, Nature (London) **462**, 628 (2009).
 - [16] J. Dalibard, F. Gerbier, G. Juzeliūnas, and P. Öhberg, *Artificial gauge potentials for neutral atoms*, Rev. Mod. Phys. **83**, 1523 (2011).
 - [17] J. Larson and E. Sjöqvist, *Jahn-Teller-induced Berry phase in spin-orbit-coupled Bose-Einstein condensates*, Phys. Rev. A **79**, 043627 (2009).
 - [18] M.-X. Huo, W. Nie, D. A. W. Hutchinson, and L. C. Kwek, *A solenoidal synthetic field and the non-Abelian Aharonov-Bohm effects in neutral atoms*, Sci. Rep. **4**, 5992 (2014).
 - [19] A. Cimmino, G. I. Opat, A. G. Klein, H. Kaiser, S. A. Werner, M. Arif, and R. Clothier, *Observation of the topological Aharonov-Casher phase shift by neutron interferometry*, Phys. Rev. Lett. **63**, 380 (1989).
 - [20] B. E. Allman, A. Cimmino, A. G. Klein, G. I. Opat, H. Kaiser, and S. A. Werner, *Scalar Aharonov-Bohm experiment with neutrons*, Phys. Rev. Lett. **68**, 2409 (1992).
 - [21] T. Bitter and D. Dubbers, *Manifestation of Berrys topological phase in neutron spin rotation*, Phys. Rev. Lett. **59**, 251 (1987).
 - [22] D. J. Richardson, A. I. Kilvington, K. Green, and S. K. Lamoreaux, *Demonstration of Berry's Phase Using Stored Ultracold Neutrons*, Phys. Rev. Lett. **61**, 2030 (1988).
 - [23] D. Frustaglia, M. Hentschel, and K. Richter, *Quantum Transport in Nonuniform Magnetic Fields: Aharonov-Bohm Ring as a Spin Switch*, Phys. Rev. Lett. **87**, 256602 (2001).
 - [24] J. W. Zwanziger and E. R. Grant, *Topological phase in molecular bound states: Application to the $E \otimes e$ system*, J. Chem. Phys. **87**, 2954 (1987).
 - [25] Y. Aharonov, S. Coleman, A. S. Goldhaber, S. Nussimov, S. Popescu, B. Reznik, D. Rohrlich, and L. Vaidman, *Aharonov-Bohm and Berry phases for a quantum cloud of charge*, Phys. Rev. Lett. **94**, 918 (1994).
 - [26] M. Svärd and J. Nordström, *Review of summation-by-parts schemes for initial-boundary-value problems*, J. Comp. Phys. **268**, 17 (2014).
 - [27] M. Almquist, K. Mattsson, and T. Edvinsson, *High-fidelity numerical solution of the time-dependent Dirac equation*, J. Comp. Phys. **262**, 86 (2014).
 - [28] J. Schön and H. Köppel, *Femtosecond time-resolved ionization spectroscopy of $\text{Na}_3(\text{B})$ and the question of the geometric phase* Chem. Phys. Lett. **231**, 55 (1994).